View metadata, citation and similar papers at core.ac.uk
brought to you by CORE
provided by Digital Repository @ Iowa State University

A NEW CONCEPT FOR A LASER-BASED ULTRASONIC PHASED ARRAY RECEIVER USING PHOTO-EMF DETECTION

D.M. Pepper, T.R. O'Meara* and G.J. Dunning
Hughes Research Laboratories
3011 Malibu Canyon Road
Malibu, CA 90265 USA
*Consultant

INTRODUCTION

The virtues of laser-based ultrasound [1], LBU, in general, and phased-array generation and detection in particular, have been appreciated for many years. The ability to improve the spatial resolution of an imaging system, coupled with the potential reduction in local laser intensity at a given location on a component to avoid surface damage while still realizing enhanced performance, represent but two motivating factors that have driven the community to seek methods by which to realize phased-array processing. There has been much activity in demonstrating that phased-array generation of ultrasound can lead to an enhanced directivity of the ultrasound as well as to a decrease (or, increase) in the bandwidth of the generated ultrasound (if desired), be it in the bulk or along the surface of components. Examples of such phased-array *generation* techniques (either in the thermoelastic or ablative regimes) include illumination of several discrete spots or locus of points with pulsed lasers [1] on the surface of a workpiece (simultaneously or sequentially), be it a line, an annular ring, or a plurality of spots—or illumination of a scanning pattern of lines along the surface of a sample, the so-called phase-velocity scanning technique [2]. By extension of the phased-array generation concept, one is led to consider the notion of laser-based, phased-array *detection* of ultrasound [3]. By reciprocity, this can lead to a receiver of higher resolution relative to a single location for the optical sensing of the ultrasound, as well as to a reduction in the local laser fluence required to achieve a given spatial performance. Moreover, one can, in principle, combine the two modes of phased-array excitation and detection to realize even greater resolution capabilities, which one may refer to as "product processing." In this case, one has, in essence, a focusing transmitter and an imaging detector, both functioning in concert.

Several groups have investigated the notion of synthetic-array processing [4, 5]. In this case, a single detector samples several locations on the surface of a part in a sequential manner. As an example, a laser beam can be raster-scanned across the surface of the workpiece, with the ultrasound signature recorded at each pixel. Upon completion of the scan, the information can be processed with the result analogous to an array of identical sensors sampling the information simultaneously. In many cases, however, it may be advantageous for a physical array of sensors to record the information in a single frame, rather than require one to dwell over the workpiece during the collection of the data by a single detector element. A natural question then arises as to why this class of enhanced receiver has yet to be realized and exploited by the community, especially in light of its myriad potential benefits. A major challenge in this regard is the receiver technology. As an example, given the success of the Fabry-Perot class of optical receiver and its inherent

Review of Progress in Quantitative Nondestructive Evaluation, Vol 17
Edited by D.O. Thompson and D.E. Chimenti, Plenum Press, New York, 1998

capability to detect ultrasound even from highly scattering surfaces (i.e., speckle) and with good sensitivity [1], it has been considered to form an array of these receivers for phased-array detection [3]. However, given the size, cost, and complexity of conventional Fabry-Perot based receivers, coupled with the fact that each such element requires an individual servo control loop for optimal performance, this solution—even though functional in principle—appears to be untractable and not cost-effective at present to realize even a modest array of such devices, say in the 50 to 100 element range.

In this paper, we propose a new concept for a non-contacting, laser-based, ultrasonic phased array receiving system. The individual elements in the array consist of nonsteady-state photo-induced emf detectors [6]. The basic element has been shown to be capable of sensing laser-based ultrasonic signals (bandwidths up to ≈80 MHz have been demonstrated), under various manufacturing conditions [7, 8]. Details of the operation of the photo-emf detector are discussed in the existing literature [6,7], and recent performance results are discussed elsewhere in these Proceedings [8]. A semiconductor-based array of such sensors can, in principle, be monolithically formed on a single substrate, resulting in a compact, low-cost, multi-pixel detector. Linear, annular, or filled array configurations are possible using this technology. In the next section, we present a description of the basic geometry of several proposed system embodiments. This is followed by simulations of an ideal array of general ultrasonic sensors, arranged in an annular configuration. We show that such an array configuration is capable of providing high spatial resolution of small hidden features, as well as the potential for electronic steering. We present the results of an ideal array (i.e., without including the particulars of the photo-emf response), since one goal of this study is to evaluate the performance of the annular array geometry, given the potential ease of its fabrication using photo-emf sensors. We show that the resolution of this particular array is comparable to that of a filled array with the same overall diameter. We also show that the array has an *afocal* property for on-axis operation, circumventing the need for precision focus adjustments. One system tradeoff involves the added side-lobe structure of the annular array. However, given that the physical fabrication (and associated cost) of the annular array is less complex relative to that of a filled array, coupled with a variety of industrial applications envisaged using this system, there appears to be potential niche opportunities for this configuration.

CANDIDATE ARCHITECTURES FOR PHASED-ARRAY DETECTION

In this section, we propose and describe two different array architectures for phased-array LBU detection: a linear array and an annular array (we discuss simulations of the latter geometry in the next section). Owing to its semiconductor-based sensor elements, the arrays can be monolithically fabricated onto a single wafer, with onboard hybrid processors. One embodiment for phased array detection of ultrasound detection is a linear array. In this case, each "pixel" in the array consists of an independent photo-emf detector element, all aligned in a single row. A lenslet array can be used to direct and collect a plurality of respective probe beams directed to and from the surface of the workpiece under test, resulting in a line of laser spots that can locally sense the ultrasonically induced surface displacements. The photo-emf array can be monolithically fabricated onto a common substrate, with parallel, programmable electronic processors provided onboard. This array can be implemented either as a reference-beam interferometer or a time-delay interferometer configuration [7].

A second example of a photo-emf array is shown in Figure 1, which shows a "beam's-eye" view of an annular array embodiment of a multi-element, photo-emf detector package. In this case, an array of photo-emf detectors is situated along a circular ring, with other concentric regions consisting of identical programmable amplifiers, filters, and other post-processing elements, with each set servicing a given photo-emf element. Each active element is illuminated with a probe and reference beam, with the fringe motion set up to move along the radial direction (alternatively, the speckle pattern from a single beam, with a given radial motion, can be sensed). This array configuration allows for a set of identical radial circuits to service the sensor elements, with a summation conductive ring at the outer region of the detector array. The entire array can be monolithically fabricated onto a

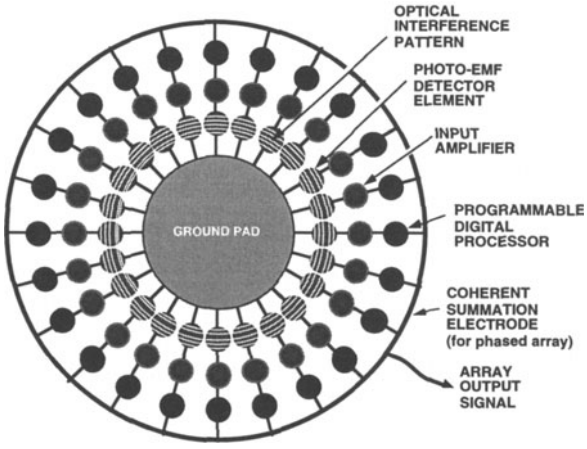

Figure 1. A "beam's-eye view" of an annular array of photo-emf detectors. Each radial spoke in the array consists of an independent detector circuit, with an optional output summing ring to generate the overall array output signal.

relatively small wafer, say 2 to 4 inches in diameter, depending on the active area and number of elements.

A typical optical system architecture using the annular array is shown in Figure 2. Here, an axicon element is used to generate a optical ring pattern that probes the surface of a workpiece. The collected light is then relayed to the photo-emf annular array through another optical train using, for example, polarization decoupling of the incident and collected beams. In the embodiment shown in the figure, a second, dual-angled axicon serves two functions: it relays the collected probe photons from the workpiece to the detector array and, secondly, it directs a coherent beam at a small conical angle relative to the probe toward the array, resulting in the desired set of circularly concentric fringe patterns. We note that an alternate geometry (not shown) can be used that employs two conventional axicons instead of the single dual-angled axicon. In this case, a slightly diverging reference beam (using one of the conventional axicons), in conjunction with the other (conventional) axicon, can be used to realize the required set of fringe patterns at the annular array plane. In either case, the interference of the pair of angularly offset conical beams forms the required set of concentric circular fringe patterns (with a grating vector in the radial direction). As before, the ultrasonically induced surface displacement on the workpiece will result in a transient movement of the fringe pattern along the radial direction at each given photo-emf detector site on the array. The output currents are then electronically directed radially outward to subsequent stages of amplification, filtering, and delay circuitry. The optical elements of this system can be packaged into a ruggedized telescopic mount for in-service operation. Polarization decoupling techniques (as shown in the figure) can be used to decouple the incident probe beam from that scattered by the workpiece. Also shown in the figure is a dichroic beam splitter, which can be used to couple a laser ultrasonic generation beam into the system co-axially with the probe beam for same-side pitch-and-catch, or pulse-echo, operation.

SIMULATIONS OF ANNULAR ARRAY DETECTION

In this section, we describe several examples of two-dimensional simulations for annular-array detection of ultrasound. In the numerical calculations that follow, we focus our attention primarily on the spatial resolution capabilities of an ideal annular array. The detailed physics and operational parameters of the photo-emf sensors are not included in this geometrical model, so that insight can be first gained into the nature of the

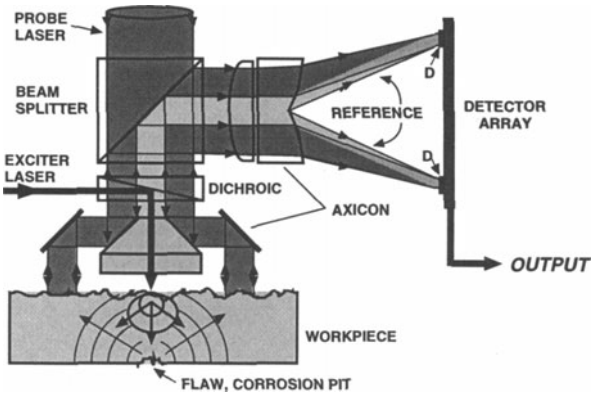

Figure 2. Example of a reference-beam interferometric architecture using the array of Figure 1.

configuration; work is under way to incorporate the operational parameters of the photo-emf sensors to gain a more realistic appraisal of this system. Given the relatively straightforward processing and fabrication steps envisioned for the annular array configuration when employing semiconductor photo-emf elements, we limit our discussion to this class of geometry in these initial studies. Figure 3 shows a drawing of a side-view of the simulation geometry. To simulate the ultrasound, we assume that a single-frequency acoustic point source exists within a given material, whose elastic properties are known. A set of laser probe spots illuminates one surface of the sample in an annular pattern, with the acoustic source positioned along its symmetry axis. In all the examples that follow, we assume that the detection is ideal (i.e., noiseless), with all elements identical. Furthermore, we limit our discussion to compression waves without mode conversion, and we also neglect other acoustic modes (e.g., surface, shear waves). The medium is assumed to be isotropic and nondispersive. Geometrical factors are included in the model, such as linear acoustic losses, as well as the projection of the compressional waves onto the surface normal in calculating the surface displacement. We also assume that the external surface of the sample has a surface figure much less than an acoustic wavelength and is therefore assumed to be ideal (i.e., flat). In reality, the surface topology must be known to within a fraction (say, a quarter-wave) of an acoustic wavelength (assuming an air interface at the boundary) or adaptive acoustical phasing approaches implemented so that high-fidelity images can be realized. Existing laser metrology systems are commercially available that can characterize the surface topology in real-time to the required specifications. Our model employs a full Huygens-Fresnel formulation of the wave propagation, and usually assumes a point detector element located at the midpoint of each photo-emf sensor location. Our mesh size consists of 271 points across the two-dimensional array area. Symmetry considerations are employed to reduce the computational time where appropriate. All our calculations were carried out using a Pentium-based PC, programmed in Basic, with conventional mathematical "recipes" used in evaluating the required integrals.

Typical results of our calculations to study the lateral resolution performance of an annular array are shown in Figures 4, 5, and 6. In these figures, we plot the point-spread function (PSF) of the system which, depending on the ratio of the detector diameter to the propagation distance from the source, would span the far-field, near-field, or intermediate range regimes. Plotted is the detected acoustic field or power as a function of lateral position along the diameter of the array across the surface of the workpiece. Linear scales are employed for all plots. In Figure 4, we plot the amplitude of the point-spread function, over a lateral range of 20 mm, for the case of a 48-element array, with an overall diameter of 20 mm, assuming a source depth of 15 mm. The speed of sound in the material is taken as 6,000 m/sec. Plotted are results for two different acoustic wavelengths, 0.3 mm (the

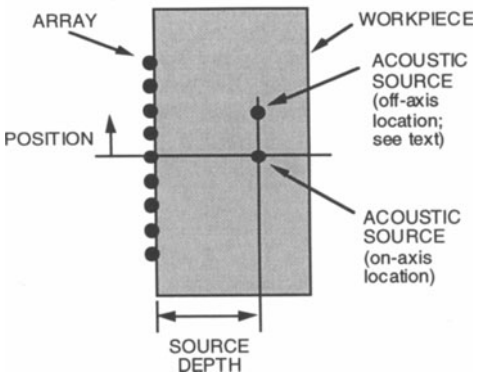

Figure 3. Basic geometry used for array simulations (side view). A buried acoustic source is placed below, and along the symmetry axis, of an ideal array of sensing locations (shown along the left-hand side of the workpiece).

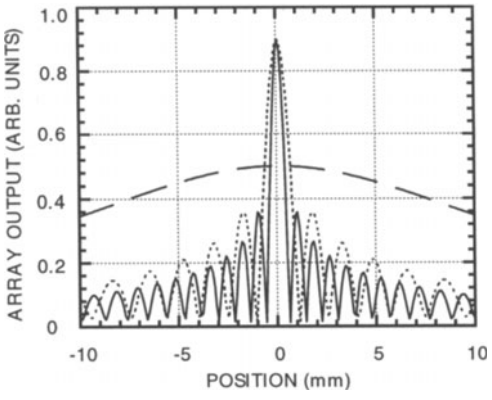

Figure 4. Point-spread function (PSF) simulation of a 48-element, 10-mm-diameter array, depicting ability to resolve lateral features of a buried source, 15 mm below the surface. Shown are results for respective acoustic wavelengths of 0.3 mm (solid curve) and 0.9 mm (dashed curve). Also shown is the PSF for a single-element detector, located at the center of the array (long-dashed curve). See text for other parameters.

solid curve), and 0.9 mm (the short-dashed curve). The respective full-width half maximum, FWHM, of the PSF for these cases is 0.46 mm, and 1.39 mm, respectively, which is on the order of an acoustic wavelength. This resolution capability is therefore on the same order of a diffraction-limited, filled array of the same overall diameter (20 mm), with the caveat that the annular array possesses more sidelobe structure. For comparative purposes, the PSF for a single-element located at the center of the array is shown (long-dashed curve), yielding a FWHM of greater than 20 mm. The annular array therefore improves the spatial resolution by more than an order of magnitude relative to a single detector element.

In Figure 5, we show the ability of a 48-element system to effectively "scan" across a feature without mechanical motion. By phasing up the output information in a programmable manner, one can electronically scan laterally across a surface without the need for relative mechanical motion. Alternatively, using parallel processing techniques, whole-field imaging can be realized simultaneously, analogous to an acoustic lens. In these simulations, the parameters are similar to those employed above, except the source depth is

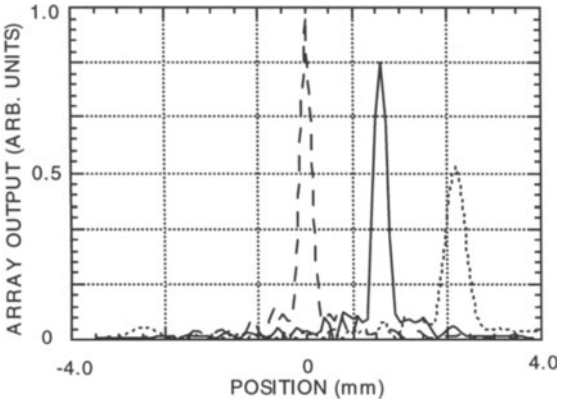

Figure 5. Point-spread function (PSF) simulation of a 48-element, 4 mm diameter array, depicting ability to electronically phase-up the elements and, therefore, to nonmechanically scan and resolve lateral features of a buried source, 4 mm below the surface. Shown are results for respective source locations on-axis (long-dashed curve), 1.6 mm off-axis (solid curve), and 3.2 mm off-axis (short-dashed curve). See text for other parameters.

now 4 mm, and the array overall diameter is 8 mm; thus, the depth-to-diameter ratio is on the same order as in the previous simulation. In the figure, we plot the acoustic power for three different phasing configurations of the detected output information. In one case (long-dashed curve), the source is positioned along the axis of the array (as in the case of Figure 3). The other two curves show how the system can be phased to respond to an acoustic source positioned off-axis, located about 1.6 mm (solid curve) and 3.2 mm (short-dashed curve) off-axis. Note that one can, in essence, view along a lateral direction across the sample without any physical motion of the array or the workpiece. The spatial resolution is seen to degrade slightly as one scans near the edge of the array. Moreover, the power level of the processed signal is essentially unaffected throughout the scan, decreasing by only 50% over the lateral extent of the array diameter. Finally, the sidelobe structure is minimal, indicating that the annular array has good lateral resolution capabilities across its diameter.

We have studied the depth-of-focus of the annular array under various conditions, as well as the ability of the system to function in the face of whole-body standing-wave modal vibrations. In Figure 6, we plot the PSF amplitude of a sparsely configured annular array system of 24 elements, for various depths of the source, assuming an acoustic wavelength of 0.3 mm for the buried source (see Figure 3 for a sketch of the simulation geometry). The simulation shows results for a relatively sparse, yet fast imaging system (maximum f/# = 1.25), with an overall array diameter of 2 mm. Note that for this simulation, the lateral position of the source ranges from being within the projection of the annular array ring, to actually being located beyond the diameter of the ring. In spite of this rather demanding set of source locations, the simulation shows that the lateral resolution varies only by about a factor of 2.5 of its minimum value—a FWHM of 0.150 mm to 0.391 mm—even as one probes into the material by over an order of magnitude in longitudinal range, from a depth of 0.25 mm to 2.50 mm, respectively. The FWHM is on the order of the acoustic wavelength over the large range of depths considered, indicating the utility of the annular array for this class of problem. We note that additional sidelobe structure appears (for the shallow-depth case) as the source position begins to overlap that of the array dimension. This so-called "proximity-lobe" structure is not surprising, considering that the source is essentially right below the one edge of the annular array, within an acoustic wavelength. We have recently studied this case, and have considered simple algorithms that can compensate for such proximity-lobes. We have also

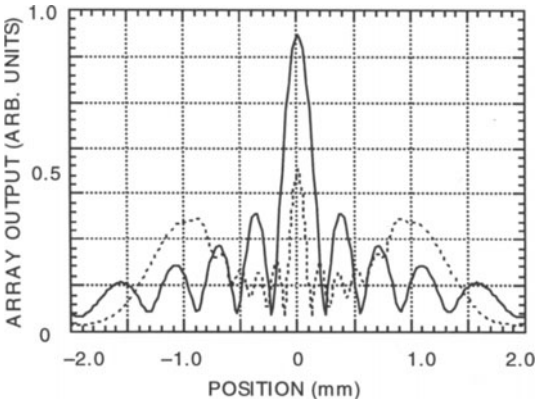

Figure 6. Point-spread function (PSF) simulation of a 24-element, 2-mm-diameter array, depicting ability to laterally resolve hidden acoustic features, buried at various depths, all along the symmetry axis of the annular array. Shown are results for respective source depths of 2.50 mm (solid curve), and 0.25 mm (dashed curve). See text for other parameters.

simulated a more densely packed and faster imaging system (maximum f/# = 0.25) with 48 elements, and found that this system maintained a FWHM within 10% of its nominal width—a FWHM of 0.145 mm to 0.162 mm, which is about one-half of the acoustic wavelength considered—again over a longitudinal range of 0.25 mm to 2.50 mm. Relative to the slower imaging system above, this system shows excellent lateral resolution capabilities, with minimal sidelobe structure over a large range of depth. We speculate that this good performance follows from the fact that the annular array mimics a Bessel-like beam [9] in a receive mode, which is well-known to maintain a non-diffractive-like behavior over a significant distance along the direction of propagation. In both cases, the annular array performance appears to be quite acceptable for many applications to image buried features.

In addition to the simulations described above, we also examined the response of the annular-array system to a scenario where, in addition to the desired (buried) ultrasound source, the workpiece is also subjected to a whole-body, standing-wave, vibration mode. It is assumed that the period of the vibration mode is less than the diameter of the annular array footprint on the sample (by about a factor of three). In general, periodic variations in the surface displacement across the face of the workpiece, when employing a single-point detector, can corrupt the LBU measurement of a desired ultrasonic surface displacement feature. In our modeling, we find that even in the face of such modal vibrations on the surface, whose period is less than the diameter of the annular array, significant spatial averaging takes place in the processed array output. This averaging of the periodic surface displacements enables one to maintain good array imaging and spatial resolution of the desired features, even in the face of such whole-body vibrations.

DISCUSSION

As with microwave phased arrays, the effective receiver beam can be scanned by mechanical motion or by receiver array element phasing (or, for broad-band operation, by timing). The scan "control" is achieved by computer processing of the detected signals rather than by optical delay lines. Although the angular scan capability is comparable to microwave arrays, this range may not be adequate for scanning of large-area thin plates. Thus, hybrid techniques, employing mechanical motion and electronic scanning may be required. Off-axis scanning permits one to achieve nearly full spatial resolution when imaging a deep scattering site near the edge of a test object, which is shown via computer

simulation of the array. The proposed array configuration is serviced by an extended laser illuminator probe beam, whose surface reflection is relayed to the array of discrete nonsteady-state photo-emf detector elements. The relay optics can also generate a coherent reference beam, required by these detectors in general. The basic low-cost detector element has been demonstrated to detect broadband ultrasonic transients, accommodate speckle generated by rough reflecting surfaces, and suppress spurious low-frequency vibrations. A monolithic, rugged detector array could be formed on a single semiconductor wafer, with on-chip electronics to accommodate most required post-processing. A variety of array configurations can be realized, ranging from a linear array, an annular (ring) array, to a filled two-dimensional array. By example, we focus our discussion to the annular array, given its simplicity of design and its good spatial resolution relative to a filled array. The array configuration reduces detector cost, simplifies reference-beam generation, and minimizes the requirement for adjusting the array timing of focus to a prescribed scattering source depth. For on-axis operation, the focusing requirement is entirely eliminated. This robust, programmable detector array may be suitable for single-frame, large-area sensing with high-spatial resolution, for such applications as the detection of buried defects (e.g., voids) in the epoxy underfill that bonds flip-chips to circuit boards [10].

ACKNOWLEDGMENTS

This work was supported by Hughes Research Laboratories IR&D funding.

REFERENCES

1. C. Scruby and L. Drain, *Laser Ultrasonics: Techniques and Applications,* (Adam Hilgar, Bristol, 1990).
2. K. Yamanaka, O. Kolosov, H. Nishino, Y. Tsukahara, Y. Nagata, and T. Koda, J. Appl. Phys. 74, 6511 (1993).
3. R.C. Addison Jr., L.J. Graham, R.S. Linebarger, and B.R. Tittmann, 1987 Ultrasonics Symposium, IEEE, 1109.
4. P. Lorraine, "High-resolution laser ultrasound imaging of Lamb Waves in thin and composite structures," Rev. of Prog. in Quant. Nondestructive Eval., Vol. 17, elsewhere in these Proceedings.
5. C. Heron, A. Blouin, F. Enguehard, J.-P. Monchalin, G. Ithurralde, and O. Petillon, "SAFT data processing applied to laser-ultrasonic evaluation of weld integrity," Rev. of Prog. in Quant. Nondestructive Eval., Vol. 17, elsewhere in these Proceedings.
6. M.P. Petrov, S.I. Stepanov, and G.S. Trofimov, Sov. Tech. Phys. Lett. 12, 379 (1986); I.A. Sokolov and S.I. Stepanov, J. Opt. Soc. Am. B10, 1483 (1993); S.I. Stepanov, Appl. Opt. 33, 915 (1994).
7. D.M. Pepper, G.J. Dunning, P.V. Mitchell, S.W. McCahon, M.B. Klein, and T.R. O'Meara, SPIE Proc. 2703, 91 (1996); G.J. Dunning, D.M. Pepper, M.P. Chiao, P.V. Mitchell, J.W. Wagner, and F.M. Davidson, Rev. of Prog. in Quant. Nondestructive Eval., Vol. 16, D.O. Thompson and D.E. Chimenti, Eds. (Plenum, New York, 1997), 579.
8. G.J. Dunning, D.M. Pepper, M.P. Chiao, P.V. Mitchell, and F.M. Davidson, "Optimizing the photo-emf response for high-speed compensation and broadband laser-based ultrasonic remote sensing," *Nondestructive Characterization of Materials VIII,* 1997, to be published; D.M. Pepper, G.J. Dunning, M.P. Chiao, T.R. O'Meara, P.V. Mitchell, I. Lahiri, and D.D. Nolte, "Characterization of the photo-emf response for laser-based ultrasonic sensing under simulated industrial conditions," Rev. of Prog. in Quant. Nondestructive Eval., Vol. 17, elsewhere in these Proceedings.
9. J. Durnin, J.J. Miceli, Jr., and J.H. Eberly, Phys. Rev. Lett. 58, 1499 (1987); D.K. Hsu, F.J. Margetan, and D.O. Thompson, Appl. Phys. Lett. 55, 2066 (1989).
10. D.M. Pepper, G.J. Dunning, M.P. Chiao, T.R. O'Meara, and P.V. Mitchell, "Inspection of flip-chip epoxy underfill in microelectronic assemblies using laser-based ultrasonic receivers," Rev. of Prog. in Quant. Nondestructive Eval., Vol. 17, elsewhere in these Proceedings.